Bachelor Graduation Project

An Acoustic Implementation of an Online Sensor Grid for Measuring Grease Deposition in Extraction Channels

E. van der Lingen, R. van Leenen

4435044, 4453530

Final Thesis

Delft University of Technology

Bachelor Graduation Project

An Acoustic Implementation of an Online Sensor Grid for Measuring Grease Deposition in Extraction Channels

Final Thesis

E. van der Lingen, R. van Leenen

4435044, 4453530

June 18, 2018

Faculty of Electrical Engineering, Mathematics and Computer Science (EEMCS)
Delft University of Technology

Delft
University of
Technology

Abstract

The cleaning company "VETkanaal"[1] requested a sensor system that measures the thickness of a grease layer within kitchen extraction ducts independently and is able to send this to an online platform. The goal of this project is to find an acoustic implementation of the sensor and be able to apply it. It appeared that measuring a shift in resonance frequencies of a plate with varying amounts of grease is the best solution for estimating the thickness of a grease layer. Afterwards, a hardware implementation was made. The conclusion of this report is that an acoustic measuring principle is certainly possible. The first tests of trying to implement such a system were moderately successful.

Contents

Preface

The project that is being described in this report is part of the final project for the Bachelor Electrical Engineering of the Delft University of Technology. The project has a duration of eight weeks. The project has been carried out by a group of six students that are responsible for the design and production of a proof of concept. The goal of this project is to identify the most promising measurement method and strategy for real time monitoring of grease deposition in extraction channels. To test this method a sensor module with electronic read-out and communication module had to be designed.

The first weeks of the project have been used to work on literature research regarding the problem. The problem definition has been defined and the program of requirements has been set up. After the research, several options for measuring methods have been tested to see which of the methods were worth investigating in more depth. It was decided that there were two different measurement implementations that were promising enough to research. At this point in time, after the first three weeks, the project group was split in three sub groups. The first group would try to develop an acoustic implementation of the sensor. The second group would develop a capacitive implementation of the sensor. The last group would be responsible for the communication module and system design of the project.

We would like to thank our supervisors Andre Bossche and Jeroen Bastemeijer for the guidance, advice and support throughout the project. Also we would like to thank Michael Kroezen and Dave Kroezen from VETkanaal[1] for their contributions to the project. Finally we would like to thank the Delft University of Technology for the available resources put at our disposal for working on this project.

Introduction

When you are cooking something, you probably are using some kind of grease to cook with. This grease evaporates, for which you might use an extraction channel to suck the evaporated grease away. Within the duct, the grease can precipitate again on the inside of the duct. If the extraction channel is short, and you do not cook a lot, this does not happen a lot. However, if you cook a lot, with a lot of fat, and have a long extraction duct, this might cause a problem. Kitchens often have a thick grease layer within their extraction ducts. This grease layer is dangerous, because it might catch fire, or worsen an already existing fire by allowing to spread through the ducts. An example of fat within an extraction channel can be seen in figure 2-1 A picture of the before and after of the cleaning of an extraction channel can be found in Figure 2-2.

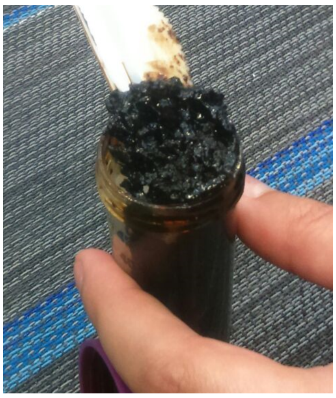

Figure 2-1: Grease found in an extraction channel

There are no guidelines on when to clean an extraction duct by the government. Some insurance companies do require of their clients that their extraction channels are regularly cleaned. Some insurance companies use a maximum thickness of 500 micron of the grease layer. The thickness of the layer is measured regularly by the cleaning company to check whether they have passed that limit or not. This is done by hand using a device that uses a pulse-echo technique [2].

Figure 2-2: Before and after cleaning of an extraction channel

The cleaning company "VETkanaal"[1] requested a sensor system that measures the thickness of the grease layer independently.

Since the thickness is currently measured by hand, it is quite resource intensive. It takes a lot of time and it requires a person at location to do the measurements. The developed sensor system should do the measurements autonomously and report the thickness indicator to a central location accessible by the extraction channel cleaning company.

2-1 Problem Definition

We are required to design a sensor system that measures the grease deposition in extraction channels of, for example, kitchens. The sensor should measure the thickness of the grease layer in order to detect when the layer thickness has reached dangerous levels and the extraction channel should be cleaned. The thickness should be available online at a central location.

This specific report will try to solve the sensor design using an acoustic sensing method. It will only solve the design of the sensor itself and not go into depth about the system design.

2-2 Outline

This report will start by describing a program of requirements given to us by VETkanaal. Firstly, some theoretical background with regards to solving the design using acoustics is provided and why acoustics was chosen to solve it. Some measurements were done to find which method would be most suitable for measuring grease thickness. The setup and results of those measurements can be found in chapter 5: Measurements. Afterwards, the design of the sensor for placement within the ducts is discussed, as well as the implementation for a final design in the chapter about System Design, chapter 6. The results of the final design are displayed in chapter 7: Results. Thereafter, a conclusion on the results is drawn in chapter 7: Results. Finally, a conclusion of the whole project is given in chapter 8: Conclusion. Lastly, the results and the outcome of the report are discussed in chapter 9: Discussion.

Program of Requirements

3-1 Introduction

In this chapter we will discuss the general system requirements and specific sensor requirements.

3-2 Safety and Environment

- The sensor should be independent of orientation, length and shape of the extraction channel. The cross-section of the channel is at least 12.5 cm.
- The sensor should work properly up to an internal temperature of the duct of 100 degrees and down to 20 degrees.
- The measurement results of the sensor should be independent of the different types of material which are used for the extraction channels.
- The cleaning of the extraction channels happens with highly alkaline chemicals; the design has to be able to either withstand or not get in contact with these chemicals.
- In order to be able to maintain the design by the current cleaning crew, the maintenance of the design should be simplistic in such a way that it can be performed by anyone who was not involved in the design process.
- The maximum distance between two sensors is 100 meters. The minimum distance is 1 meter.

3-3 Performance

- The measurement results should be independent of the temperature.
- The consistency of grease deposit differs per site and per extraction channel. The sensor should work for every form of grease deposit.

- The sensor should be able to measure and quantify the thickness of grease in an extraction channel.
- The sensor should quantify at least a level where the thickness is considered dangerous.Usually a level of 500 micron is considered dangerous.
- The sensor should have a lifetime of at least one year (the sensor should be working until the next time of cleaning).
- The range of interest, in which the sensor is able to measure accurately, is from 0 to 600 micron.
- The accuracy of the measurement results should be within ± 30 μm within the range of interest.
- The sensor should not influence the even grease deposition in the extraction channel.

3-4 System Design

- Up to a maximum of 8 sensor per system can be used.
- The measurement results should be displayed on an online platform.
- The production cost should be in line with the costs of an extraction channel.

3-5 Laws and Ethics

- The sensor design should differ from the already existing patent on grease measurement [3].
- The responsibility for the time to clean the extraction channel will be at the cleaning company.

Theoretical Background

4-1 Measurement Methods

Some research has been done to look into several methods of how to measure the grease layer thickness. First of all, it was investigated how thickness of layers in general is being measured right now as well as at current designs for measuring grease in any form. In the end a conclusion was made on which methods are most suitable for the current project.

There were several methods using optics to measure thickness. The first method using optics focused on ellipsometry: [4] [5] [6] [7]. There have also been methods that look at infrared, or near infrared light to determine fat within food or humans [8] [9]. Other methods also looked at the opacity of the material to use [10]. This method is also the one implemented in the already existing patent [3]. Using optics is not very useful as sensor within the duct, because it requires an antenna and a receiver, which would be hard to implement in all kinds of different shapes of ducts.

The second possibility is to measure grease layer thickness using acoustics, where the difference in speed of sound in two materials can be used to derive more properties of one of the materials. In this paper, resonance frequency and signal decay change with fouling layer thickness [11]. There were multiple methods that use acoustics to measure oil thickness and bodily fat as well [12] [13].

Thirdly, methods using inductive measurements [14], capacitive [15], or conductive [16] are possible. These methods all have in common that the properties of the fat will most likely differ a lot for each extraction channel. Most notable is capacitive, since the other methods are more affected by the fact that the duct is made from metal.

Making use of a fourth method one can also measure using electromagnetic radiation [17] [2]. This is quite complex, and requires a setup which is hard to make in an extraction duct.

Last but not least, one can also measure using thermal measurements. By knowing the inside temperature of the duct, estimation of the thickness can be done by knowing the outside temperature as well. [18] [12].

A measurement method that is not too difficult, is not invasive on the testing environment and will be most likely to be accurate enough to perform the measurements is needed. The final decision was to look at a capacitive measurement method, as well as an acoustic measurement method, since they fit these requirements best.

4-2 Wave propagation in solids

With equation 4-1 it is possible to find the resonance frequency of a vibrating plate. In this equation v_s is the speed of sound in a material and λ is the wavelength. The speed of sound also depends on the Young's modulus of solids and the Bulk modulus for fluids and density. Equation 4-2 can be used to determine this value. One can see that the speed propagation in a material depends on the density and therefore the acoustic speed changes in different materials.

$$f = \frac{v_s}{\lambda} \tag{4-1}$$

$$v_s = \sqrt{\frac{B}{\rho}} = \sqrt{\frac{Y}{\rho}} \tag{4-2}$$

In section 5-4 one can see the measurements for determining the speed of sound in copper, stainless steel and brass. In these measurements the following equation is used to find the speed in materials 4-3. For brass the speed will be 4070 m/s, for copper it is 4605 m/s and stainless steel has a speed of sound of 5469 m/s, see section 5-4.

$$x = v_s * t \tag{4-3}$$

4-3 Plate resonance theory

From the speed of sound is it possible to find the frequency, if you know the wavelength λ. However, there are more than only the calculated resonance frequencies. From figure 4-1 one can see that the resonance patterns become very complex when the frequency increases. There also exist formulas for vibration at a resonance frequency. However, these equations become to complex and depend on many things and are out of the scope of this study [19]. In section 5-5 there is a short experiment of how the resonance patterns look like in a copper plate.

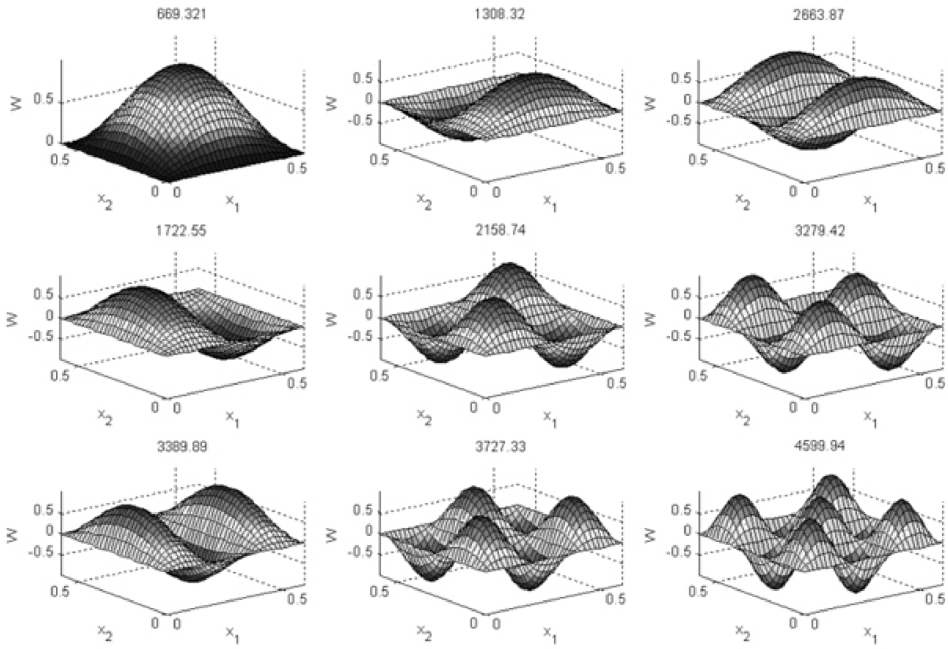

Figure 4-1: Patterns of wave attenuation at different frequencies [20].

Measurements

5-1 Introduction

In this chapter you will find the experiments done to come to a conclusion for the final design of the sensor.

5-2 Measurement 1: Proof of Concept

The goal of this experiment was to proof that the concept of acoustic measurements would work, and the method itself had value pursuing.

5-2-1 Setup

We placed a piezo speaker on the outside of a steel duct and another one on 3 cm distance. The duct had a thickness of 1 cm and a diameter of 25 cm . We put a $5V_p - p$ sine to one piezo, on a frequency between 4 and 5.5 kHz. We received the signal from the other piezo and let the oscilloscope perform a Fast Fourier Transform (FFT). For every frequency we noted the power of the signal at that frequency. We did this for both a sweep between 4 and 5.5 kHz with 100 Hz between each measurement, as well as between 4.5 and 5 with 50 Hz between each measurement.

Then several layers of masking tape were applied, and the experiment started again. The masking tape was used as substitute for grease, since real grease was not available at this point.

These measurements were done twice and an average was taken.

5-2-2 Results

The results of the first measurements can be seen in figure 5-1. The results of the second measurement can be seen in figure 5-2. Note that below -58 dB, background noise has a significant influence.

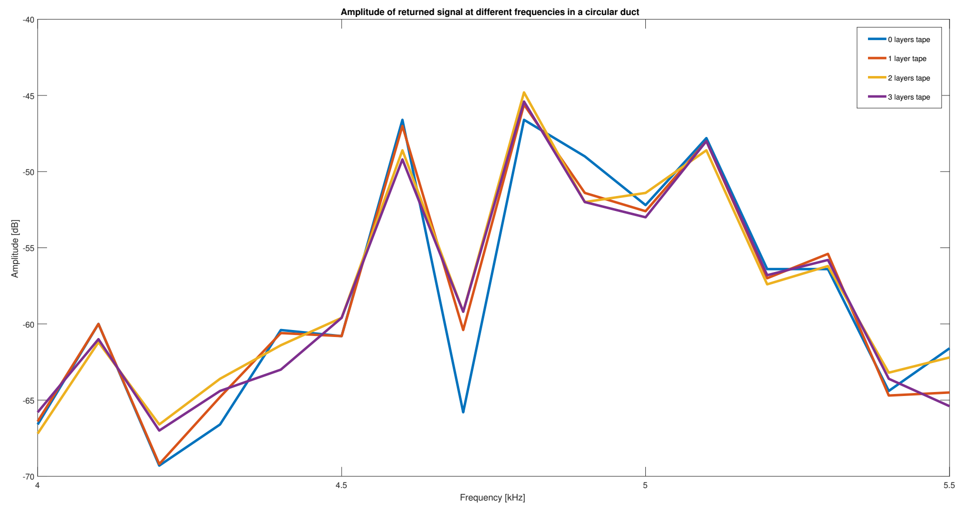

Figure 5-1: Measurement 1.1: Frequency sweep between 4 and 5.5 kHz

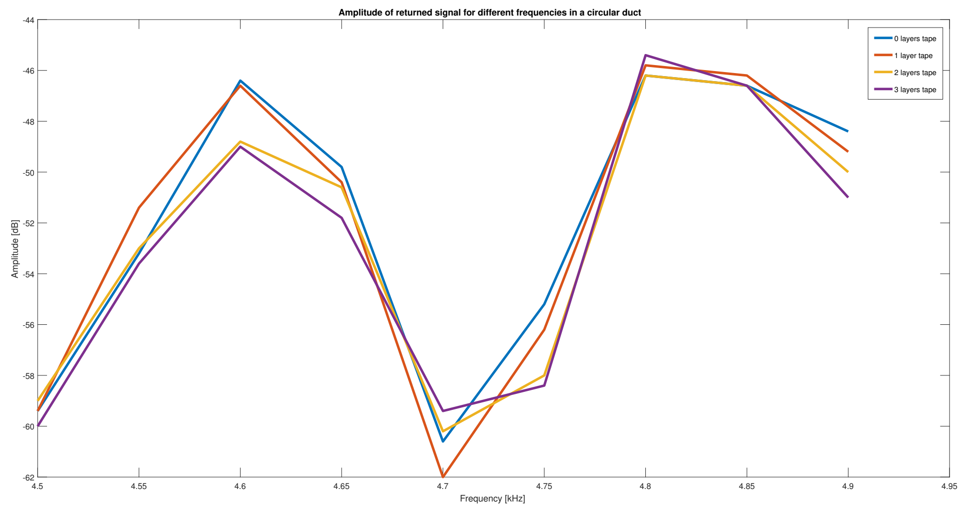

Figure 5-2: Measurement 1.2: Frequency sweep between 4.5 and 5 kHz

5-2-3 Conclusion

The results of the proof of concept showed promise for future measurements. At some frequencies there is a clear relation between the received amplitude and the amount of layers of tape. It does not show any shifting frequencies yet.

Although the measurements were successful, the method definitely needed improving. The coupling between the (flat) piezo's and the (round) duct, was bad, which caused very low signals. The Fourier Transform on the oscilloscope is slow and difficult to handle. Furthermore, we used tape instead of real grease, which means it is still unclear if it really works for grease as well.

5-3 Measurement 2: Large Plate

The goal of these experiments was to prove the correlation between layer thickness and whether received attenuation would still hold up for real grease, and improve our method of measuring the frequency response.

5-3-1 Setup

A $30x30x0.15cm$ steel plate was used and two piezo's were placed in the center at a distance of 4 cm of each other, see figure 5-3.

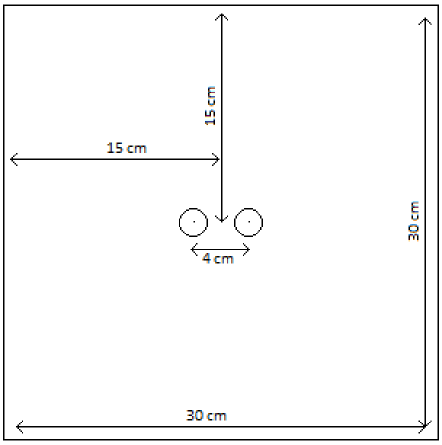

Figure 5-3: Measurement 2: Setup

Through one piezo a $10V_p - p$ sine wave frequency sweep was sent, which went through 3 to 6 kHz in 20 ms. The returning signal from the other piezo was sampled at 48kHz by a PC soundcard and an FFT performed in Matlab using the script found in appendix A-1-1.

Several layers of masking tape were applied around the plate. The area within the tape was filled in with real fat and any surplus was scraped off, so the grease would have a thickness equal to the masking tape.

5-3-2 Results

The result of the experiment can be found in figure 5-4.

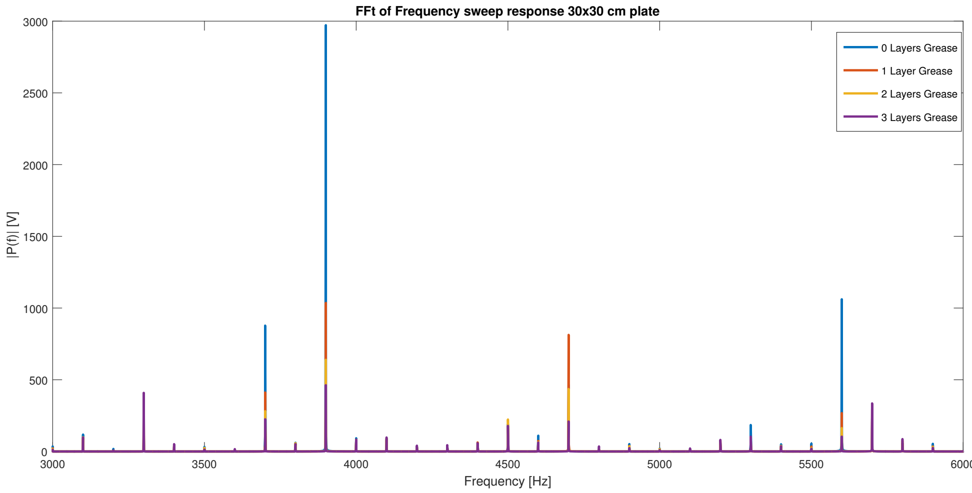

Figure 5-4: Measurement 2: A frequency sweep on a 30x30 cm plate

5-3-3 Conclusion

The results of this experiment further proved that an acoustic measuring method is most certainly possible. At 3.9 kHz a clear loss of attenuation can be measured for more layers of tape.

What also can be seen is that the function generator used to generate the signal is not perfect. The generated frequencies are discrete and not continuous. Therefore, it is unclear if resonance frequencies are shifting or just disappearing.

After the experiment the piezo's were shifted around the plate a bit and adjusted their distance between each other. This causes a massive change in where the resonance frequency is. This means some resonance pattern exists on the plate, which may be used as an advantage. Because this is an important factor in designing the sensor, further tests with regards to resonance patterns have been done (see sections 5-4 and section 5-5).

5-4 Measurement 3: Speed of Sound in Metals

In chapter 4 it is mentioned that every material has a different speed of sound. The goal of this experiment was to determine the speed of sound in different materials and hence make it possible to find the resonance frequencies.

This was done to find out more about resonance on plates to possibly use resonance patterns as an advantage when trying to measure from a plate.

5-4-1 Setup

For this experiment the following devices were used:

- Single Channel Arbitrary/Function Generator (AFG3021C) [21].
- Two channel Digital Storage Oscilloscope (TDS2022C) [22].
- Two piezo speakers [23].
- Copper, steel and brass plates of 7x14x1.5 cm, see figure 5-5.

These specific materials were used because copper is quite soft and will have a low speed of sound, steel is quite hard and will have a high speed of sound, and brass because its an alloy.

The piezo speakers which are used for this setup differ from the piezo's of section 5-2 and 5-3. These piezo's [23] have a better performance and especially in the frequency range of 15 kHz up till 45 kHz. With the function generator a pulse of 10Hz was put on one piezo. The other piezo receives the delayed signal. This signal is examined on the oscilloscope.

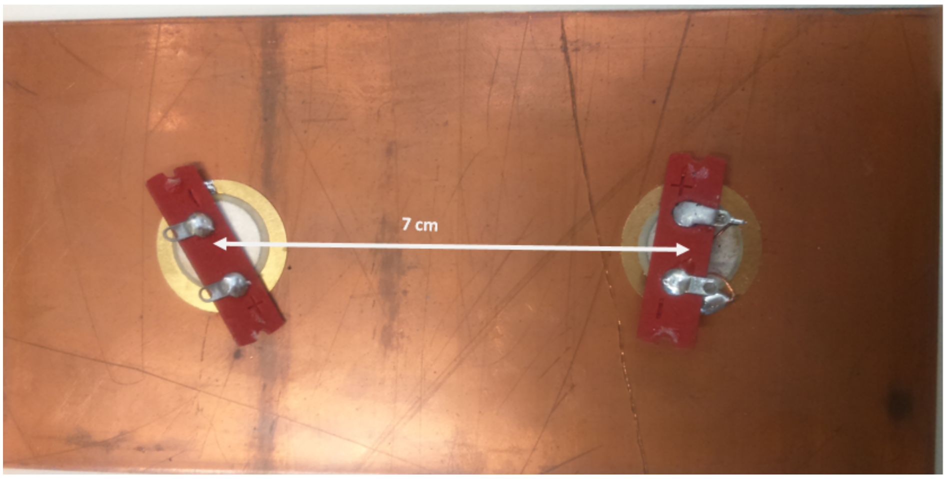

Figure 5-5: Copper plate with piezo's used for experiments.

5-4-2 Results

Figures 5-6, 5-7 and 5-8 display the time delay noted at cursor two. Figure 5-5 shows that the distance between the two piezo's is 7 cm. From equation 4-3 the velocity can be determined.

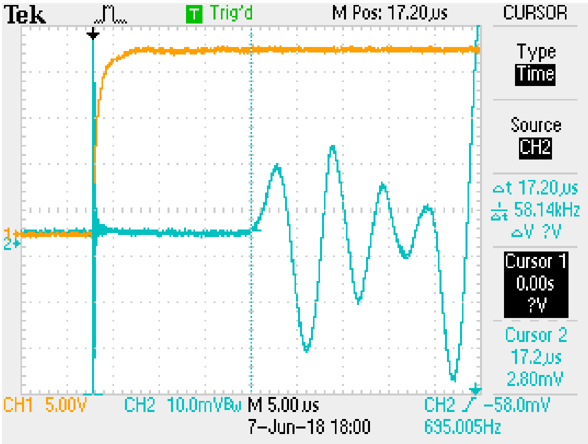

Figure 5-6: Time delay in brass.

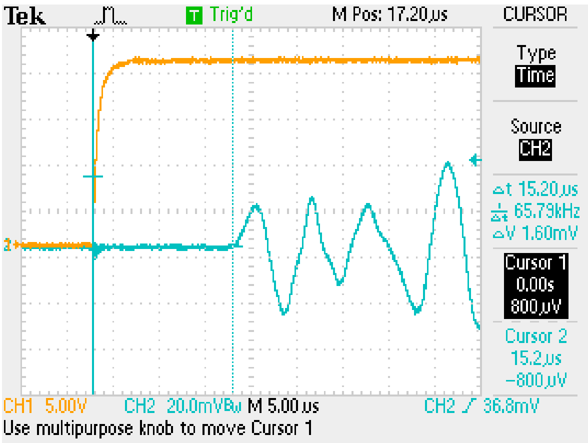

Figure 5-7: Time delay in copper.

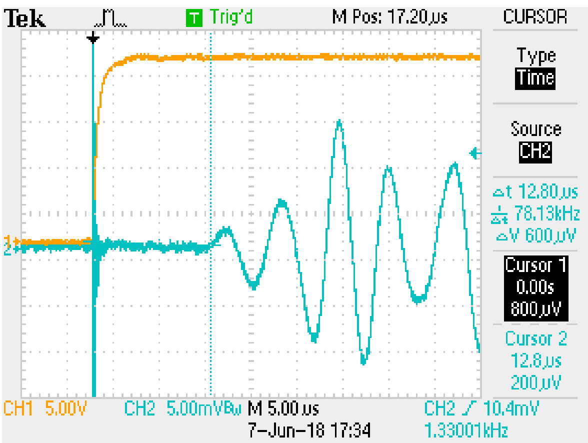

Figure 5-8: Time delay in steel.

5-4-3 Conclusion

The results show for brass that the speed propagation will be 4070 m/s, for copper 4605 m/s and steel has a speed of sound of 5469 m/s. For steel the speed propagation should be around the 5790 m/s, for copper it should be between 3560 - 3900 m/s and for brass it is between 3500 - 4700 m/s [24]. So, the measurements are almost the same as the expected value of the speed of sound in these materials. However for brass the speed propagation differs. This is possible, because brass exists of different types of materials and does not always have the same composition.

5-5 Experiment 4: Resonance Pattern on Small Plate

The goal of this experiment was to find the resonance pattern for a copper sheet.

5-5-1 Setup

The devices that are used for this experiment are as follows:

- Single Channel Arbitrary/Function Generator (AFG3021C) [21].
- Copper sheet of 14x7x1.5 cm, see figure 5-5.
- Salt.

With the function generator a Sine AC signal was sent to the piezo and the copper plate vibrates, the salt on the plate will move to the places where the plate vibrates least, so a pattern might display.

5-5-2 Results

Figure 5-9 shows the resonance pattern of a copper sheet at a frequency of 18.3 kHz.

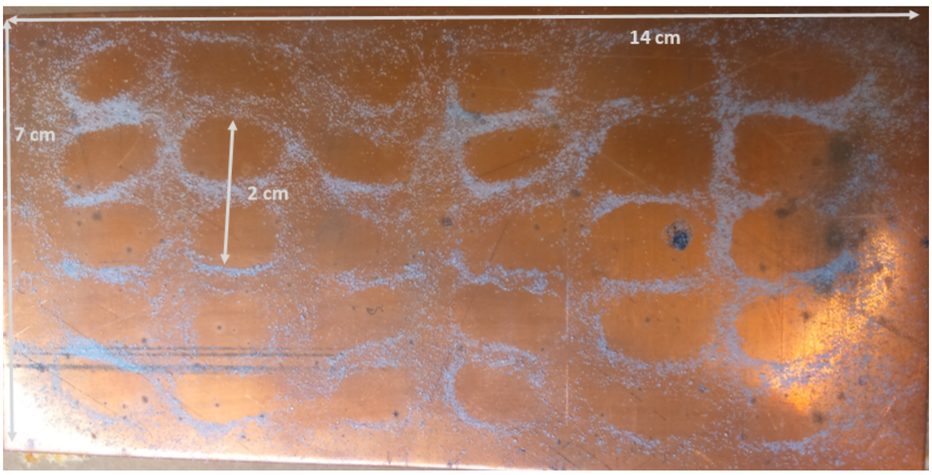

Figure 5-9: Resonance pattern on a copper sheet.

5-5-3 Conclusion

Figure 5-23 clearly shows a resonance frequency in copper at 18.3 kHz, meaning resonance patterns do exist at resonance frequencies. On the 14 cm side of the plate one can see that there are 3.5 wavelengths, which states that $\lambda = 4$ cm. For the short side of 7 cm one can see that the wavelength λ is 2 cm. From formula 4-1 the frequency can be calculated and shows that this will be around 230 kHz for λ =2 cm. It is clear that this is not the frequency the pattern was created with.

From this experiment one can conclude that at a frequency of 18.3 kHz a clear resonance pattern exists. However, this is not true for every frequency, because waves interfere with each other and at frequencies that are not resonance frequencies, no pattern will appear. It can also be seen that the pattern is quite complex. Perhaps the most important to note is that the wavelength λ seen on the resonance pattern is not corresponding to the frequency the pattern exists at. It is probably at a multiple of 18.3 kHz, but this is hard to determine accurately. Therefore, due to the unpredictability of the resonance patterns, it is difficult to take resonance patterns into account when designing the placement of the piezo's on a plate.

5-6 Experiment 5: Small Plate

The goal of this experiment was to find a correlation between the grease thickness and the phase and attenuation of the received signal from the piezo.

5-6-1 Setup

For this experiment the same setup as in section 5-5 was used. However, there are also steel and brass sheets, which have the same dimensions as the copper sheet and the piezo's are put on the same places, see figure 5-5. Different thicknesses of grease were applied on the sheets. For the steel sheet the extraction channel grease and deep frying fat were used for the measurements. The copper and brass sheets were only measured with deep frying fat.
There was chosen for deep frying fat and not extraction channel grease, because deep frying fat is easier in use and has almost the same measurement results as the extraction channel grease (this can be seen in the steel results).
With Matlab the signal of the receiving piezo is recorded and a simulated lock-in amplifier is used to determine the phase and attenuation, see figure 5-10. The reference signal used for this lock-in amplifier came from the function generator. However, this sine AC signal frequency sweep had a V_{pp} of 10 V. The computer could not record this signal, so a voltage divider was used to reduce the amplitude to a value of 1 V. The returning signal from the other piezo was sampled at 192kHz by the PC soundcard. In figure 5-10 is A the real part of the signal and B the imaginary part. The attenuation then will have a value of

$$\sqrt{A^2 + B^2}$$

and the phase will have a value of

$$\arctan(\frac{B}{A})$$

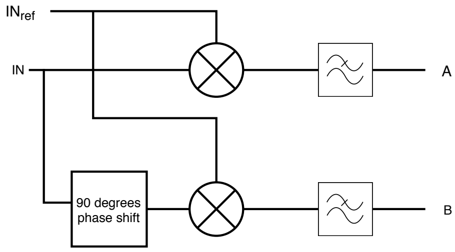

Figure 5-10: Simulated lock-in amplifier used for Matlab.

Furthermore, these measurements are done with the different type of sheets. For the Matlab code, with the simulated lock-in amplifier, see appendix A-1.

5-6-2 Results

Firstly the results of the attenuation and phase of the steel sheet are discussed, with extraction channel grease and deep frying fat. Secondly the measurements of the brass sheet and lastly the measurements of the copper sheet.

Steel

The measurements with the extraction channel grease will be discussed regarding attenuation and phase. Subsequently, the measurements with deep frying fat will be discussed regarding the attenuation and phase.

Extraction channel grease (attenuation measurement)

Figure 5-11 shows the attenuation of the frequency sweep of the steel sheet. The figure shows strong peaks at different frequencies, these frequencies are the resonance frequencies of the plate. On these peaks one can detect the difference between the grease thickness.

For a clarification a zoomed-in version can be seen in figure 5-12, at a frequency of 3.4 kHz.

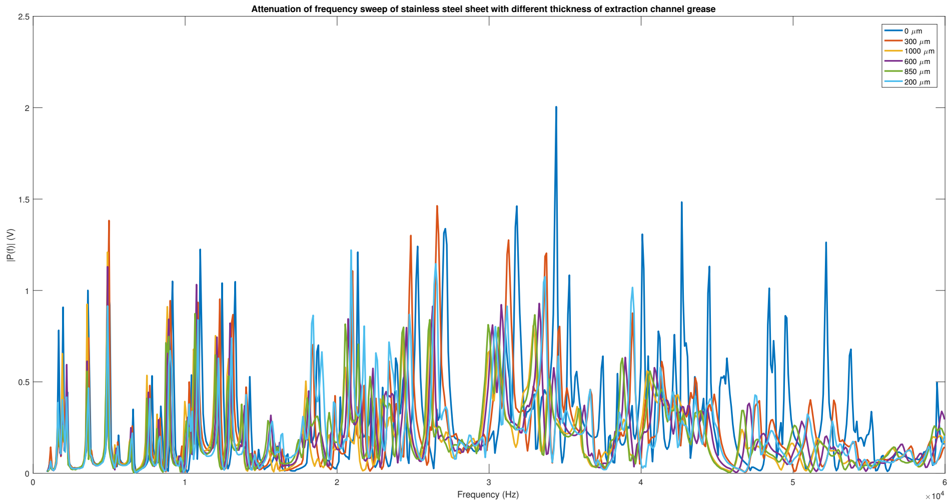

Figure 5-11: Attenuation of frequency sweep of steel sheet with different thickness of extraction channel grease.

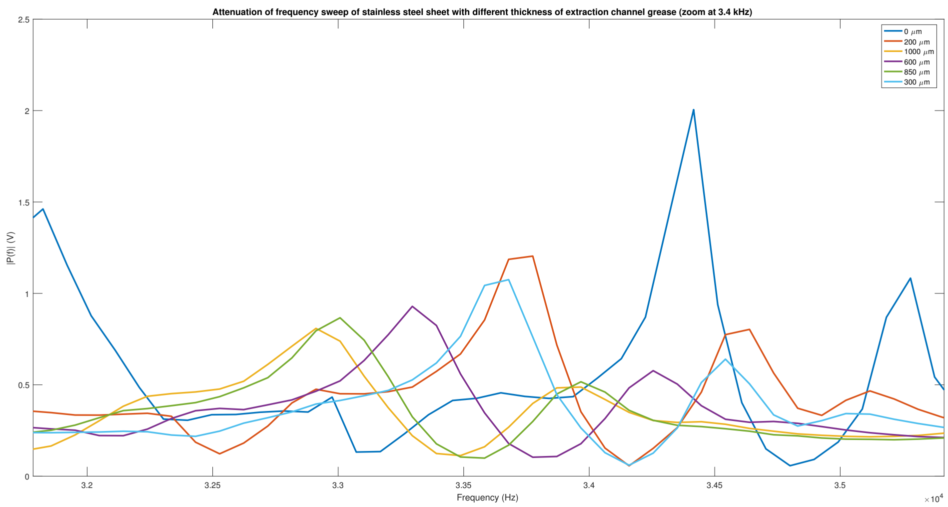

Figure 5-12: Attenuation of frequency sweep of steel sheet with different thickness of extraction channel grease (zoomed in at 3.4 kHz).

Extraction channel grease (phase measurement)

Figure 5-17 shows the phase response of the frequency sweep of the steel sheet. For a clarification a zoomed-in version can be seen in figure 5-18, at a frequency of 3 kHz.

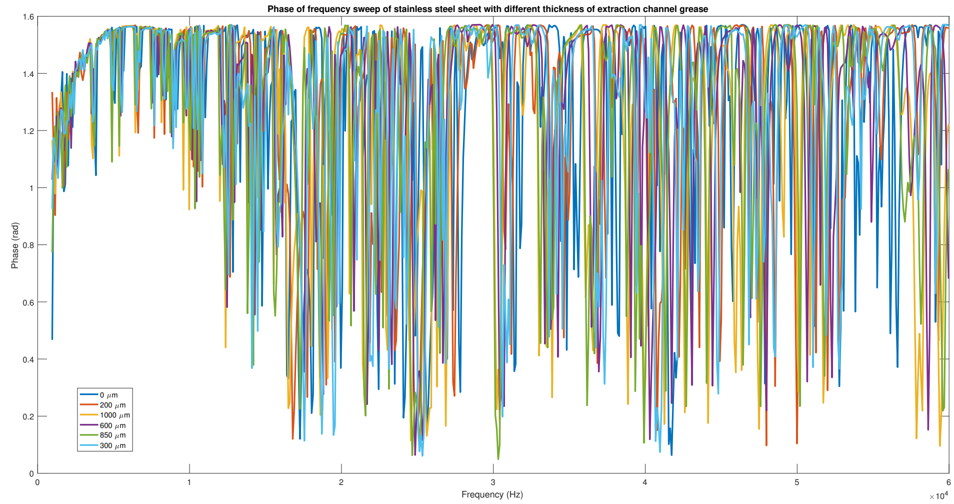

Figure 5-13: Phase of frequency sweep of steel sheet with different thickness of extraction channel grease.

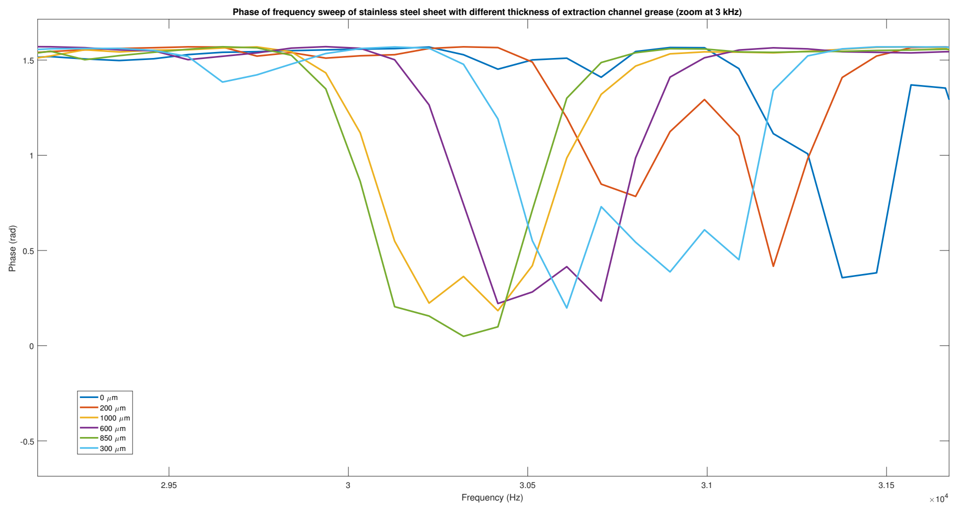

Figure 5-14: Phase of frequency sweep of steel sheet with different thickness of extraction channel grease (zoomed in at 3 kHz).

Deep frying fat (attenuation measurement)

Figure 5-15 shows the attenuation of the frequency sweep of the steel sheet. For a clarification a zoomed-in version can be seen in figure 5-16, at a frequency of 3.4 kHz.

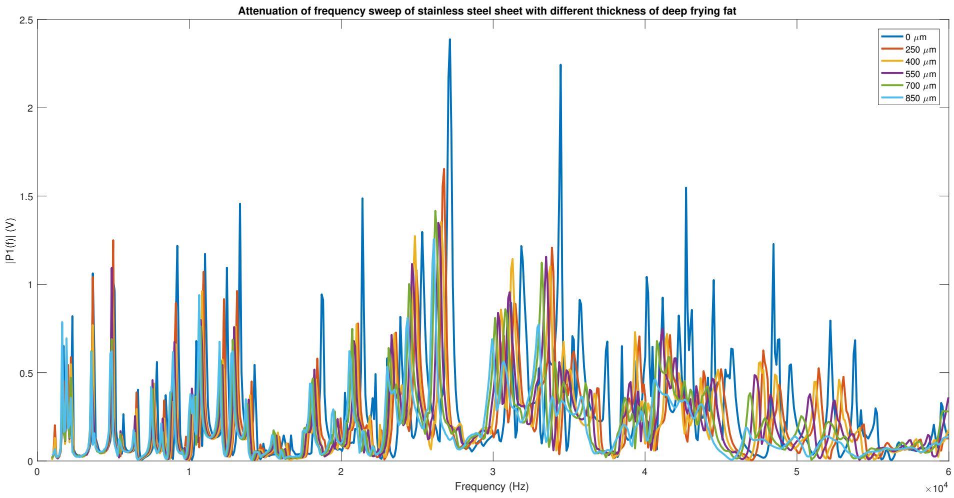

Figure 5-15: Attenuation of frequency sweep of steel sheet with different thickness of deep frying fat.

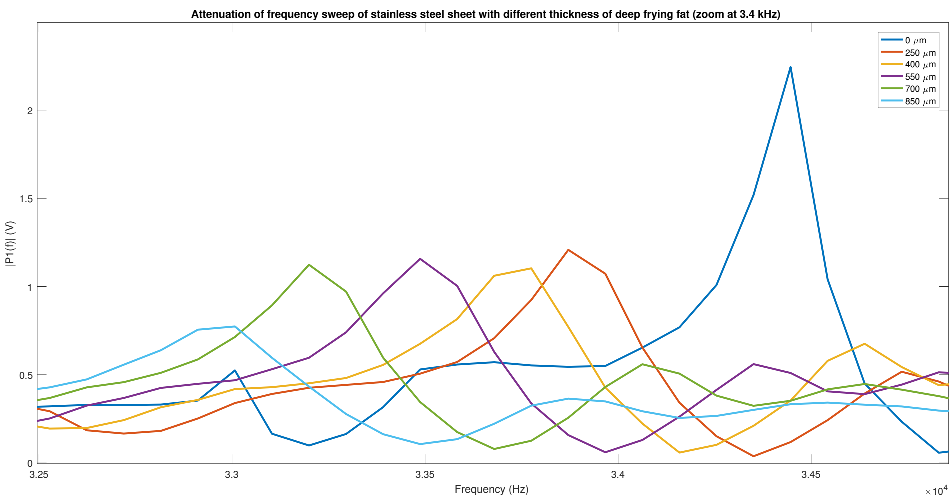

Figure 5-16: Attenuation of frequency sweep of steel sheet with different thickness of deep frying fat (zoomed in at 3.4 kHz).

Deep frying fat (phase measurement)

Figure 5-17 shows the phase response of the frequency sweep of the steel sheet. For a clarification a zoomed-in version can be seen in figure 5-18, at a frequency of 3 kHz.

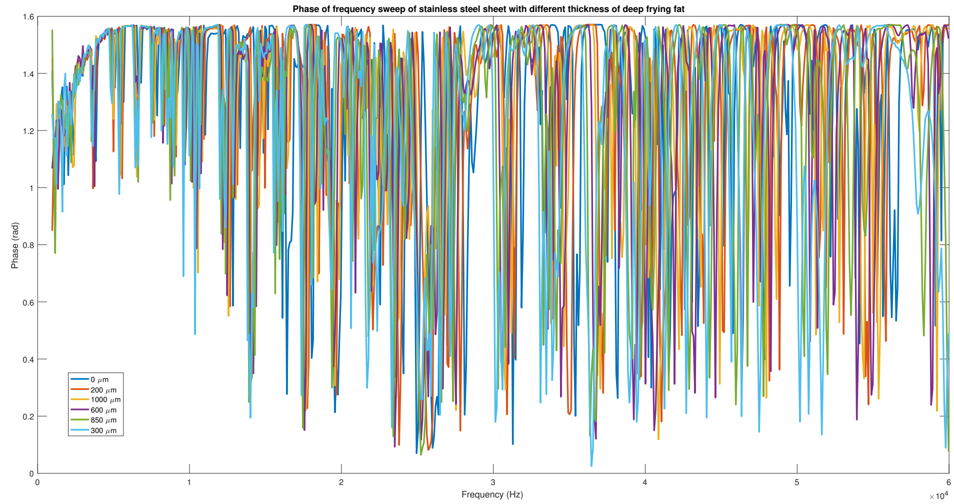

Figure 5-17: Phase of frequency sweep of steel sheet with different thickness of deep frying fat.

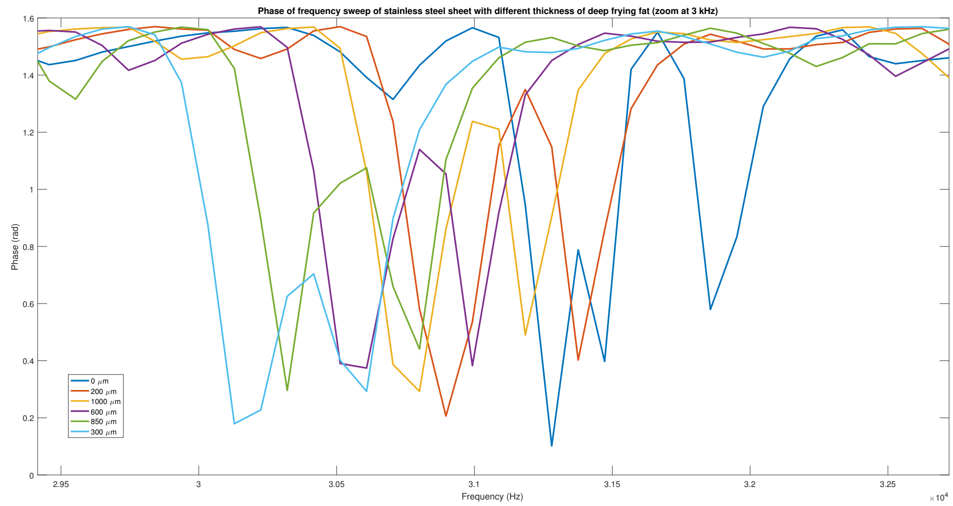

Figure 5-18: Phase of frequency sweep of steel sheet with different thickness of deep frying fat (zoomed in at 3 kHz).

Brass

First the attenuation measurements will be discussed and secondly the phase measurements of the brass sheet.

Attenuation measurements

Figure 5-19 shows the attenuation of the frequency sweep of the brass sheet. For a clarification there is a zoomed-in version of figure 5-19 at a frequency of 3.26 kHz. This can be seen in figure 5-20.

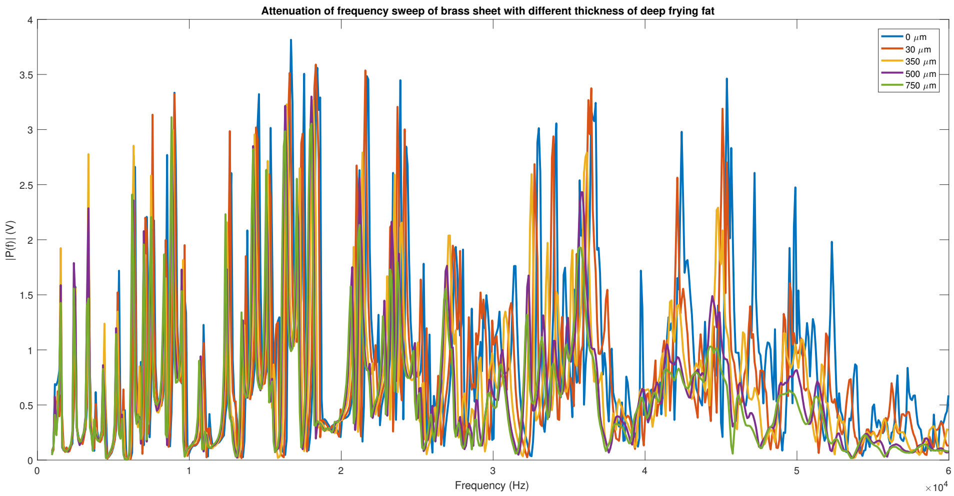

Figure 5-19: Attenuation of frequency sweep of brass sheet with different thickness of deep frying fat.

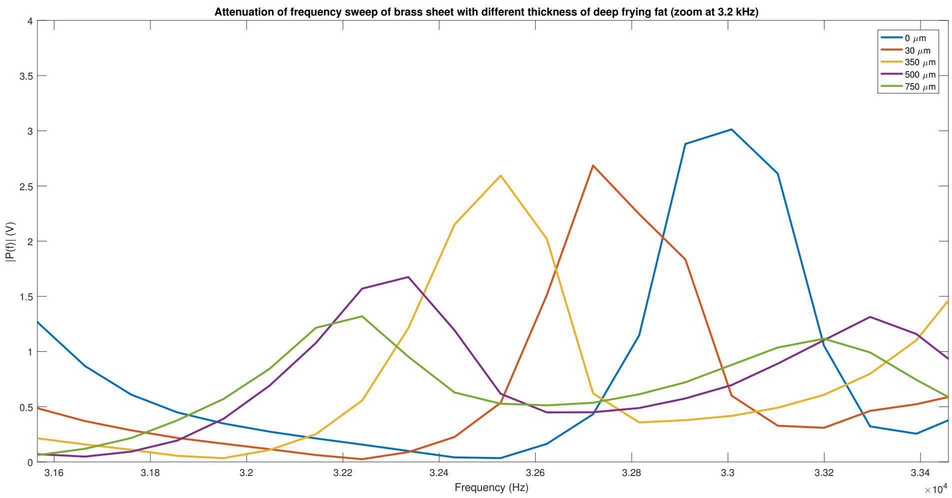

Figure 5-20: Attenuation of frequency sweep of brass sheet with different thickness of deep frying fat (zoomed in at 3.26 kHz).

Phase measurements

Figure 5-21 shows the phase response of the frequency sweep of the brass sheet. For a clarification there is a zoomed-in version of figure 5-21 at a frequency of 3.2 kHz. This can be seen in figure 5-22.

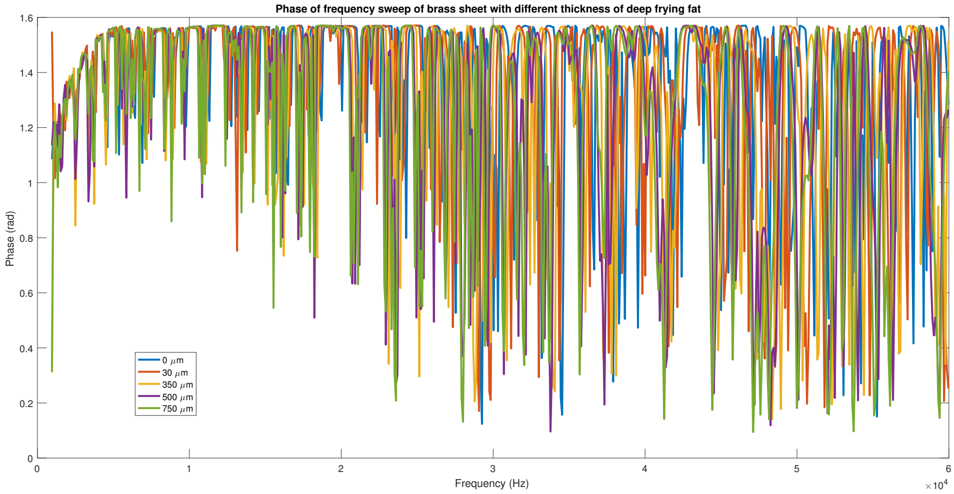

Figure 5-21: Phase of frequency sweep of brass sheet with different thickness of deep frying fat.

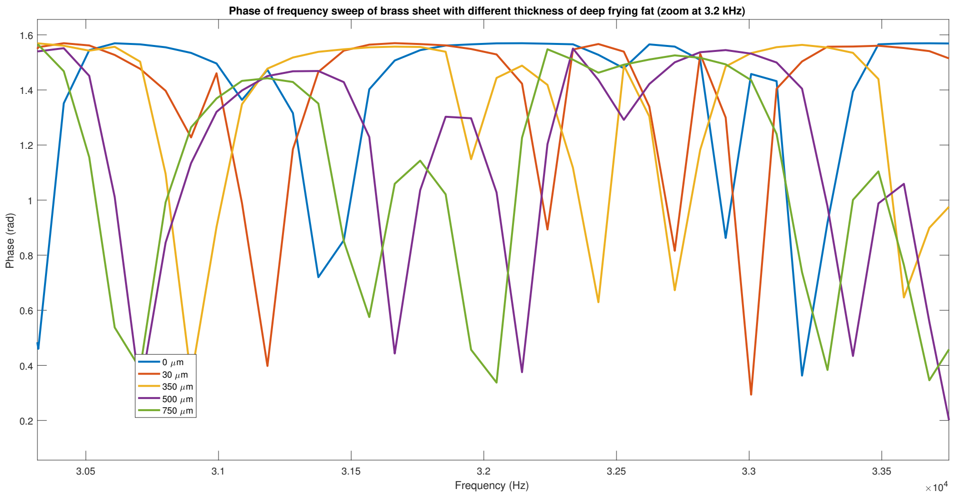

Figure 5-22: Phase of frequency sweep of brass sheet with different thickness of deep frying fat (zoomed in at 3.2 kHz).

Copper

First the attenuation measurements will be discussed and thereafter the phase measurements of the copper sheet.

Attenuation measurements

Figure 5-23 shows the attenuation of the frequency sweep of the copper sheet. For a clarification there is a zoomed-in version of figure 5-23 at a frequency of 3.26 kHz. This can be seen in figure 5-24.

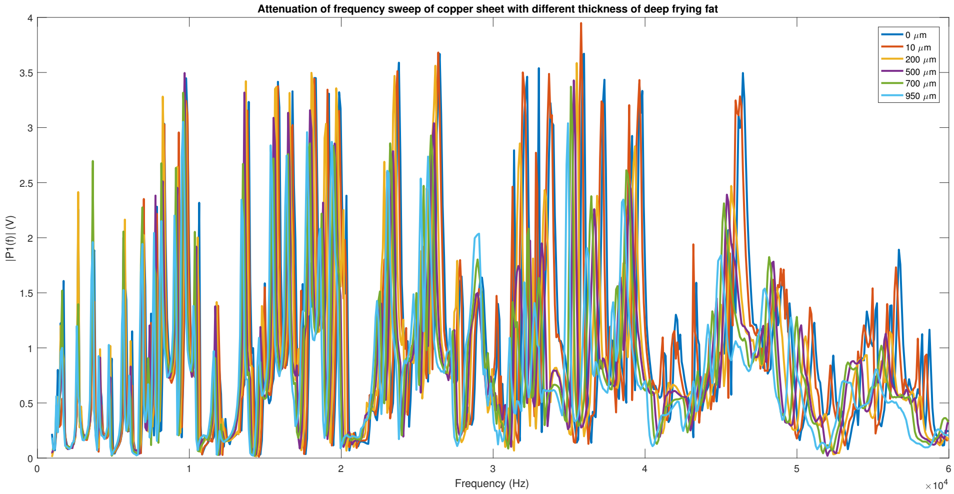

Figure 5-23: Attenuation of frequency sweep of copper sheet with different thickness of deep frying fat.

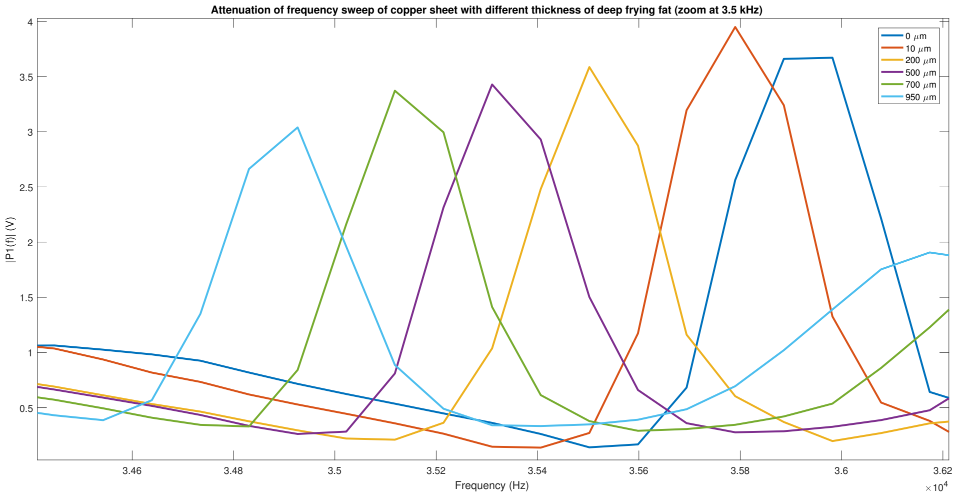

Figure 5-24: Attenuation of frequency sweep of copper sheet with different thickness of deep frying fat (zoomed in at 3.5 kHz).

Phase measurements

Figure 5-25 shows the phase response of the frequency sweep of the brass sheet. For a clarification there is a zoomed-in version of figure 5-25 at a frequency of 4 kHz. This can be seen in figure 5-26.

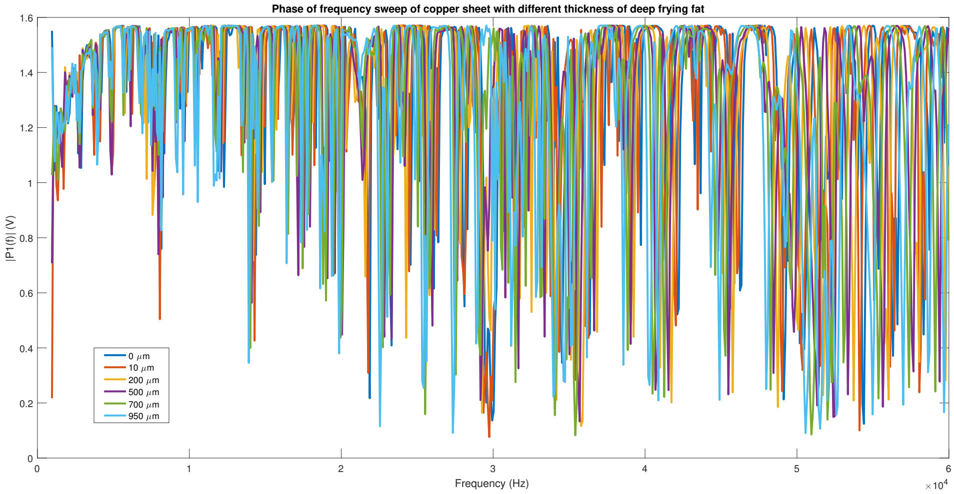

Figure 5-25: Phase of frequency sweep of copper sheet with different thickness of deep frying fat.

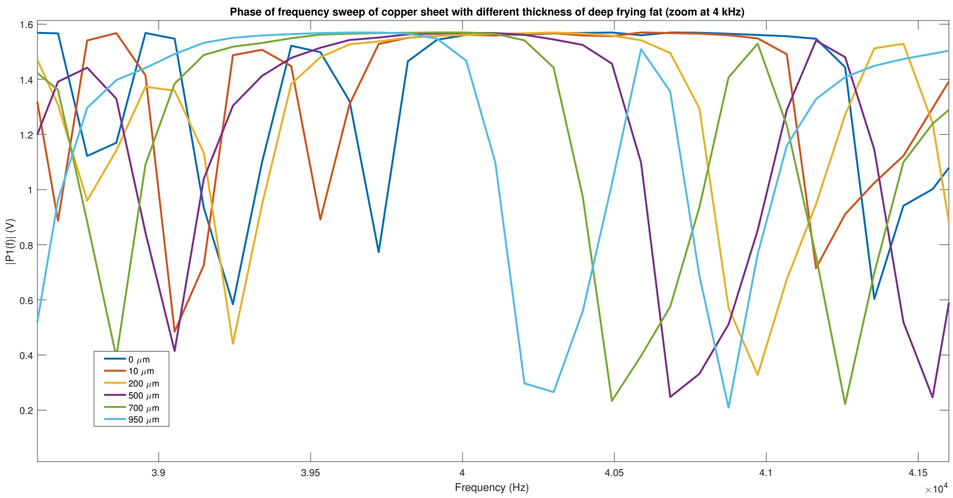

Figure 5-26: Phase of frequency sweep of copper sheet with different thickness of deep frying fat (zoomed in at 4 kHz).

5-6-3 Conclusion

Looking at the phase, resonance frequency shift and attenuation, one can conclude that the phase detection is not useful for grease thickness detection, because the phase has several values for a small range of frequency. These changes are to fast and are therefore difficult to detect.

Besides the decline of attenuation, the signal also shows the resonance frequency shifting to the left when the grease thickness increases. The zoomed-in figures show clear frequency shifts when the grease thickness increases. This is only clear at high frequencies. Attenuation therefore is reliable, because the changes are large enough to detect and a relation between the grease thickness and attenuation can be found.

Frequency shift detection is also a reliable method for detecting grease thickness. The figures in section 5-6 show that there is a correlation between the frequency shift and the grease thickness.
From these measurements a correlation can be seen in the grease thickness and the frequency shift. A formula can be found and from this formula is it possible to find the right frequency by the right grease layer thickness.

Lastly, the measurements on steel regarding the extraction channel grease and deep frying fat are almost the same besides the frequency shift. However, the shifts are less for extraction channel grease, but the difference is still detectable. Therefore the assumption can be made that deep frying fat can be used as another type of grease for easier handle.

System Design

6-1 Prototype

When the cleaning company (VETkanaal) wants to clean the extraction channels, they make a hole in the duct. Then they are able to remove all the grease from the inner duct and after cleaning, a hatch is used to close the duct again.

In this way it is possible to implement the acoustic design on the hatch, so that the electronics can be removed from the duct when cleaning is necessary. This implementation can be seen in figure 6-1.

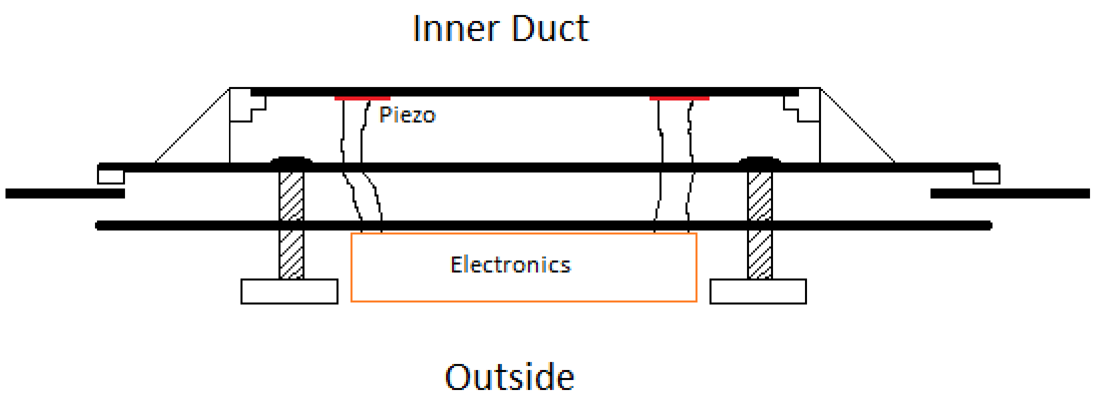

Figure 6-1: Design implementation in the duct.

The 7x14 cm material sheet with the piezo's, see figure 5-5, will be put on the inner side of the hatch and therefore will be in the inner duct. With wires through the hatch the piezo's will be connected to the outside of the duct and on this side of the hatch all the electronics will be attached. How the electronics will get their supply voltage will be discussed by the subgroup communication.

6-2 Implementation

6-2-1 Measurement Method

From the graphs displayed in the final measurement procedure (see section 5-6), the decision was to make a system based on a change in resonance frequencies. There were several other options to choose from, each of them explained below:

With regards to the phase, it gets really messy, and there is no specific frequency in which the phase moves up or down at a predictable rate. There are some frequencies for which the phase moves predictably, but choosing a frequency at which there is enough range to cover all layer thicknesses and still not move into regions where the phase moves unpredictably, is impossible.

Static frequency attenuation measurements face about the same problem, although the attenuation is not nearly as messy as the phase. At some frequencies there is a really nice relation between layer thickness and attenuation. There is a large difference between testing the attenuation at a single frequency at low frequencies, and at high frequencies:

The problem with static frequency measurements at high frequencies is that the resonance peaks usually decay quickly, and on the sides of the resonance peaks there is not a lot of difference to be seen between the frequency responses at different layer thickness. Therefore, the shifting of resonance frequencies at high frequencies and using that property to look at the attenuation at a static frequency around these resonance frequencies would not work. You could also use a low number of static frequencies, and derive the thickness from the attenuation at those frequencies, but then you are kind looking at shifting resonance frequencies anyways.

The problem with static frequency measurements at low frequencies is that the accuracy at thick layers of grease is very low. This is a good option though, but especially for small layers of grease.

The next option are dynamic frequency measurements. This means doing a frequency sweep of some sort, and using certain properties to derive the layer thickness.

The first option is about the same as static frequency measurements at low frequencies, but now dynamically at high frequencies. This method would entail finding the resonance peak, and use the height of that resonance peak. This faces the same problem as with static frequency measurements, the accuracy at small layers of grease is quite low.

The second option of using dynamic frequency measurements would be to find the resonance peak, and using the location of the resonance peak to derive the layer thickness. This is, of course, only possible at high frequencies. There are some great examples in the frequency domain where this method could be used. The accuracy of these measurements is great, both at low, as well as large layer thickness. The only downside is that it is harder to implement than using a static frequency.

Dynamic frequency measurements and use the location of the resonance peak to derive the layer thickness were used. This was the best option, but required some extensive hardware to be built. The system built to find and analyze resonance peaks has been described below. The decision was made to use the resonance peak at around 36 kHz (and lower afterwards) in the copper plate, see figure 5-24. These peaks are well spaced out, have little interference from peaks near it and are high enough to easily measure. This specific set of frequencies was not based on hard science, but a set of peaks was taken that looked alright.

6-2-2 System Overview

The entire system was developed in association with the other subgroups. A specific subgroup will design the communication and power supply for our sensor. An overview of this general system can be found in figure 6-2.

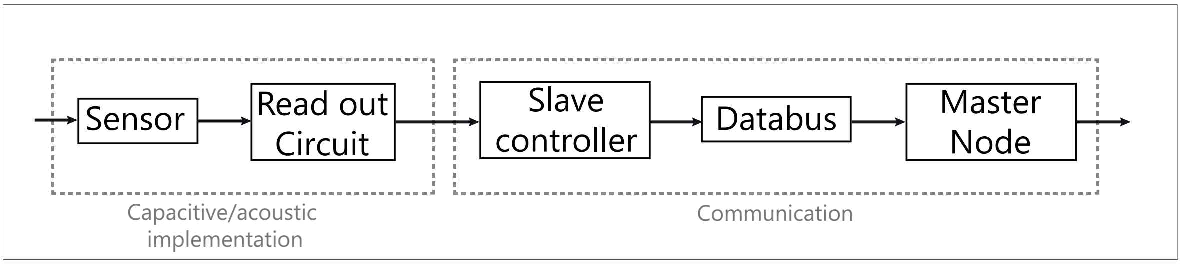

Figure 6-2: General System Overview

The entire system overview can be found in figure 6-3.

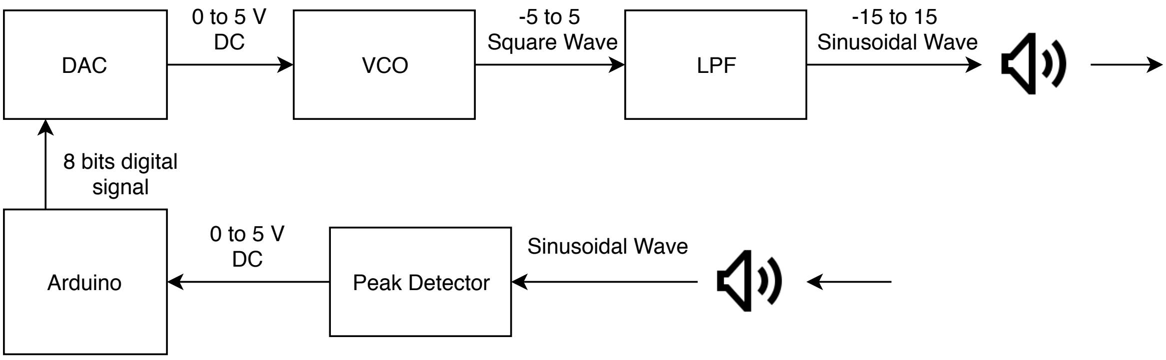

Figure 6-3: System Overview

The first challenge which need to be faced is making a sine wave at a high frequency, with an adjustable frequency, at such a power that it could drive a piezo with a high resistance and high capacitance, and produce sufficient signal at the receiving piezo speaker too and reduce noise influence.

The Arduino (see chapter 6-2-7) will send an 8 bit signal to a Digital Analog Converter (see chapter 6-2-3), because the Arduino does not have a DAC itself. The DAC controls a Voltage Controlled Oscillator (VCO) (see chapter 6-2-4), which is able to make a square wave form at frequencies given by the input voltage. A Low Pass Filter is used to make a sine wave from the square wave (see chapter 6-2-5) and provide the correct power and voltage specifications to drive the piezo.

The second challenge is to read a heavily distorted sinusoidal signal and determine the attenuation from it. The attenuation information should be fed back to the Arduino.

A simple peak detector (see chapter 6-2-6) is used to determine the peak value of the signal, and provide it in a good format to the Arduino.

The third challenge is that the frequency which the VCO delivers is temperature and supply voltage dependent. This was fixed by feeding the input from the VCO back to the Arduino, so that the Arduino can analyze the frequency that is being generated. (This connection is not displayed in figure 6-3)

Most of the following designs required some sort of amplifier. Most of the amplifiers had to meet some specifications, so an one-fits-all solution was used. The amplifier should have a high slew rate to make sure it can handle the combination of high frequency and high voltage. It also needed to have low harmonic distortion at 36 kHz as well as be able to drive strange loads like the piezo (especially regardign load capacitance). The used amplifier is the MC33078 [25]. It has a high slew rate and still functions properly at 36 kHz. It can also be used for high quality audio applications, so it will be able to drive strange loads like the piezo.

6-2-3 Digital Analog Converter

The DAC used, was the DAC0800LCN/NOPB [26]. This is a fairly standard 8-bits DAC, and its circuit can be found in figure 6-4.

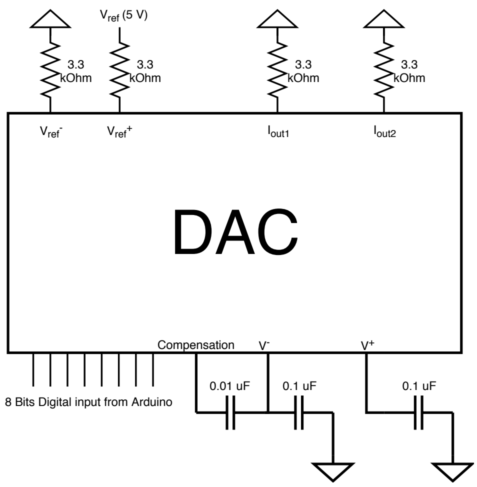

Figure 6-4: DAC Circuit.

At the non-inverted output of the DAC there is a voltage follower and after that an inverting voltage-voltage amplifier to get the voltage in the correct way for the VCO.

6-2-4 Voltage Controlled Oscillator

There has been chosen to do a frequency sweep, so a Voltage Controlled Oscillator (VCO) is necessary to translate voltages to square wave signals with different frequencies, which are determined from the voltage of the digital analog converter, see section 6-2-3.

The component used for the VCO is the CD74HCT4046AE [27]. The resistor of 55 kΩ is used for the frequency offset of 34.8 kHz. The capacitor and the resistance determined the frequency range of the VCO. There is chosen for a frequency range of 34.8 kHz up till 36.2 kHz. From the figures given in the data sheet, the values of the capacitor and resistor became 45.2 nF and 22 kΩ.

The output signal of the VCO (0 up till 5 V) will become the input of the LPF. However, the output signal of the VCO was not a clean square wave, because there was a lot of distortion on the higher portion of the square wave. To reduce this internal noise, there has been chosen for an amplifier with hysteresis [25] (+15 and -15 V) to make a more clean square wave. With the help of a voltage divider, a square wave of -5 to 5 V is sent to the LPF.

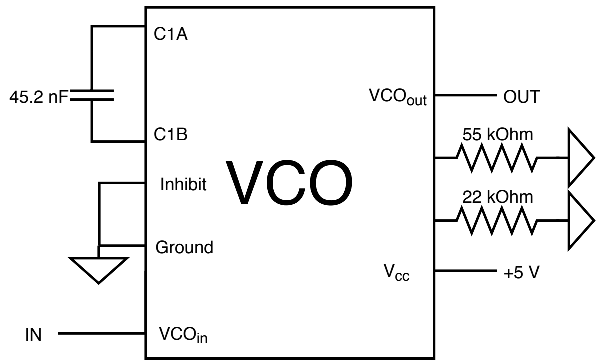

Figure 6-5: Voltage controlled Oscillator implementation

6-2-5 Sine Generator - Low Pass Filter

A Sallen-key filter is chosen as low pass filter for the square waveform [28], with a voltage-voltage amplifier with an amplification of 2. The resistors and capacitors can be calculated from formula 6-1. The cut-off frequency is chosen at 45 kHz and $R_1 = R_2$ and $C_1 = C_2$. The components then will be $R_1 = R_2 = 10k\Omega$ and $C_1 = C_2 = 330pF$.

$$f_c = \frac{1}{2\pi\sqrt{R_1 R_2 C_1 C_2}} \tag{6-1}$$

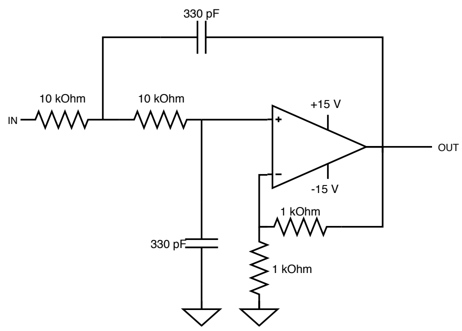

Figure 6-6: Low pass filter implementation.

6-2-6 Peak Detector

The peak detector circuit is fairly simple. When the signal voltage is larger than present on the capacitor, the capacitor gets charged. However, the capacitor also slowly gets discharged by the resistor in parallel.

The threshold voltage of the diode is countered by placing an amplifier over it. The circuit can be viewed in figure 6-7.

The value of the resistor and capacitor was chosen based on the decay time τ of the RC couple. With a τ of 15 ms, the RC circuit has enough time to respond to a new peak, especially at higher frequencies. The values of the resistor and the capacitor were chosen accordingly.

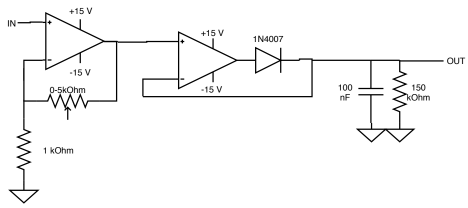

Figure 6-7: Peak detector implementation.

The maximum voltage at the output of the peak detector for this frequency range is about 2 V, which could be amplified to fit the input range of the Arduino better, but this is not done because at other frequencies the output could reach over 5 V.

6-2-7 Arduino Integration

The Arduino used is an Arduino Uno (3rd Rev.) [29]. This Arduino is powerful enough to perform all functions needed for this project and has enough pins to connect to the system.

The Arduino has 3 main functions:

- Putting data on the digital pins, so the DAC can transform it into an analog signal.
- Reading the signal from the peak detector.
- Measuring a frequency from the VCO, for frequency confirmation.

All of these functions are discussed below.

Digital Output

The function $findpeakfreq()$ is responsible for handling the frequency sweep and finding the peak frequency and calls most other functions. The function *puttodigipins*() is the specific function that dissects the integer it has been given, and puts the correct value in binary on the pins 3 to 10, with 3 being the least significant bit.

Reading Analog Input

Another function is $doanameas()$ which is the function that measures the input from pin 5, to which the peak detector is connected. Doanameas takes 20 samples of the value on the analog pin and averages it. The integer as argument given to this function determines how often it should run these 20 sample bits. It returns the complete average of the bit value read on the pin. This value is a double, but still represents a bit value between 0 and 1024. Since conversion to a real voltage is not necessary, it is not done.

Measuring Frequency

Measuring frequency on an Arduino is easy, but not for high frequencies, like in this case. The maximum sampling time of the ADC is at topmost 8.9 kHz. Not nearly enough to measure a 36 kHz signal. There is a workaround though. The function $makeFreqMeting()$ implements the frequency measurement.

The ADC only functions at a frequency of 1 MHz as a maximum. At such a high frequency, it has a worse accuracy than at lower frequencies. The ADC uses a prescaler to scale the standard clock frequency of the Arduino (16 MHz) back to an amount fit for the ADC, in which it has a good accuracy. This prescaler is standard 128, which means the ADC standard runs on about 125 kHz. So, with the ADC at a frequency of 125kHz, the maximum sampling frequency is 8.9 kHz.

The datasheet of the micro controller of the Arduino (the ATmega328) [30], describes the way of changing the prescaler for the ADC. The prescaler we used was 4, meaning the frequency the ADC runs on is 4 MHz. This gives a massive boost to the sample frequency, but due to the nature of the Arduino it is still not constant so timing the program is still needed.

The frequency measurement starts by taking 300 samples. The time it takes to get those samples is timed in microseconds, with an accuracy of 4 μs. Afterwards, the sampled space is scanned for rising clock edges and falling clock edges. The frequency is derived from the fact that there is one rising clock edge and one falling clock edge in one period.

The frequency measurement is repeated corresponding to the argument given to the function and an average of all measurements is returned.

Results

In this chapter the results from the subsystem will be discussed and also the result from all the subsystems working together. The subsystems and the entire system can be seen in section 6.

7-1 Results per Subsystem

Every subsystem is tested separately from each other. These results will be discussed in this section.

7-1-1 Digital Analog Converter

The DAC works accordingly as presented in the system design. The conversion is linear with no noticeable deviation.

7-1-2 Voltage Controlled Oscillator

With a programmable DC power supply, a DC voltage will be set on the VCO input. This voltage can be adjusted in such a way that a corresponding square wave with corresponding frequency will be generated. This signal is investigated on the oscilloscope [22] and can be seen in the follow figures 7-1 and 7-2.

Figure 7-1 shows the output of the clipping amplifier with an VCO input voltage of 0V. The corresponding f_{min} can be seen as 30.85 kHz. This value differs from the value in section 6-2-4, which has a value of 34.8 kHz. This is possible, because the figures in the datasheet, from which you should read the value of R1, R2 and C1 are not very accurate.

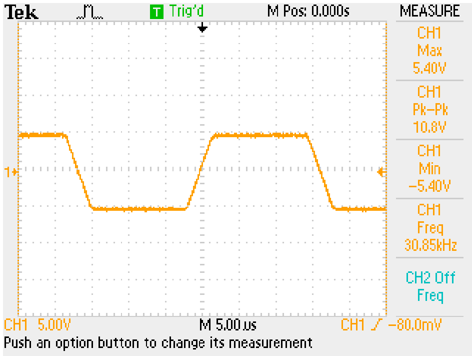

Figure 7-1: VCO output with hysteresis amplifier with an input voltage of 0V.

Figure 7-2 shows the output of the amplifier with hysteresis with a VCO input voltage of 4.7V. The corresponding f_{max} can be seen as 44.78 kHz. This value differs from the value in section 6-2-4, which has a value of 36.2 kHz for the same reason as described above. What also can be seen is that the slew rate of the amplifier is met. This actually does not matter, since the frequency is not affected, and the signal is used to create a sinusoidal waveform anyways.

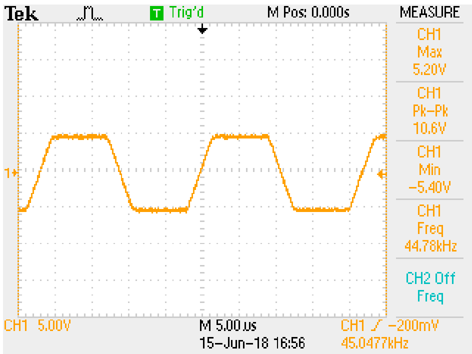

Figure 7-2: VCO output with hysteresis amplifier with an input voltage of 4.7V.

To conclude, the VCO works properly in the used frequency range of 34.8 till 36.2 kHz. Although the frequency range of the VCO differs from the designed frequency range, the range can still be adjusted by a suitable voltage interval, which corresponds to the range of frequencies.

7-1-3 Sine Generator - Low Pass Filter

With the function generator [21], an AC square wave (10 V_{pp}) will be sent to the input of the low pass filter. This square wave can be adjusted in frequency in such a way that a corresponding sine wave with the same frequency will be generated. This signal is investigated on the oscilloscope [22] and can be seen in the figures 7-3 and 7-4.

Channel 1 in figure 7-3 shows the input signal from the function generator[21] and channel 2 shows the corresponding output signal of the sending piezo on the oscilloscope [22]. Channel 2 shows a signal which looks almost like a sine wave and has a V_{pp} of around 30 V.

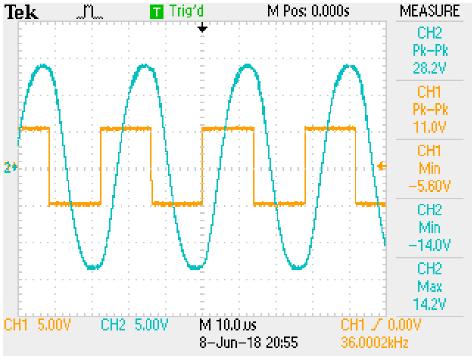

Figure 7-3: Low pass filter output signal send to the piezo.

Channel 1 in figure 7-3 shows the input signal from the function generator and channel 2 shows the corresponding output signal of the receiving piezo. Channel 2 shows a signal which looks almost like a sine wave and has a V$_{pp}$ of 4 V

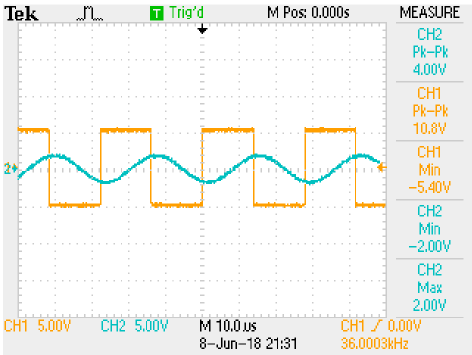

Figure 7-4: Low pass filter output signal received from the piezo.

To conclude, The LPF works accordingly as presented in the system design, see section 6-2-5. It works very good for the frequency range it is supposed to work on, namely 34.8 up till 36.2 kHz, delivering a sinusoidal signal.

7-1-4 Peak Detector

The peak detector works accordingly as presented in the system design. It works very good for the frequency it is supposed to work on, delivering a signal with a very small AC component.

In figure 7-5 the input and output for a 10 V_{pp} sine at 31 kHz can be seen. The peak detector delivers a signal with a small (0.16 V_{pp}) AC component. The average of the signal, 4.64 V is close enough to the actual value of 5 V.

In figure 7-6 the input and output for a 10 V_{pp} sine at 1 kHz can be seen. Because the frequency is quite low, the drop-off between the peaks is larger and brings a larger AC component (0.32 V_{pp}). However, at this frequency, the peak detector is better able to follow the peaks and reach the top value of the peak, before the peak drops off. Therefore, the average is closer to the actual value: an average of 5.04 V compared to the 5 V that was put into the peak detector.

In figure 7-7 the input and output for a 0.4 V_{pp} sine at 36 kHz can be seen. This figure proves the circuit still works properly, even for low voltage and high frequency. The AC component is about 0.24 V_{pp}, and an average of 0.16 V compared to the 0.2 V it should be.

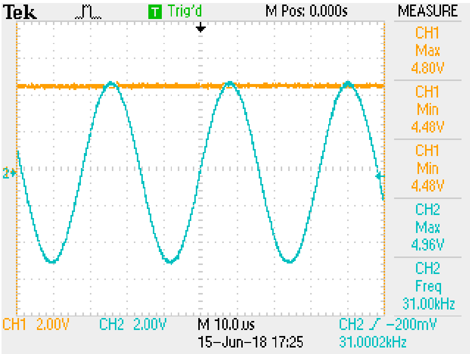

Figure 7-5: Peak detector input and output at 31kHz and $10V_{pp}$.

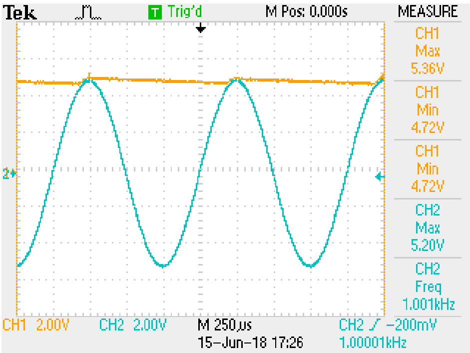

Figure 7-6: Peak detector input and output at 1kHz and $10V_{pp}$.

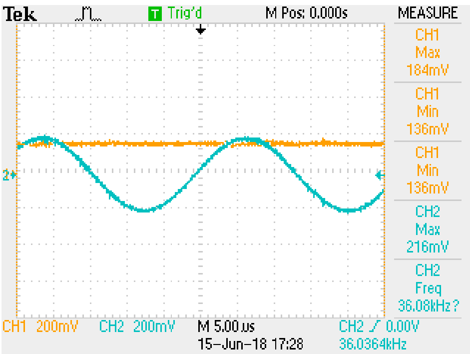

Figure 7-7: Peak detector input and output at 36kHz and $0.4V_{pp}$.

7-1-5 Arduino Integration

The digital output of the Arduino functions as expected. The settling time (the time between sending the command and before the proper values have appeared at the output gates) was a bit high, so the delay before the measurements could be done was increased.

The reading of the analog input also functions properly.

The frequency measurement does not function exactly as intended. There is a deviation between the frequency that is being put in, and the frequency the Arduino determines. This deviation is constant for a constant frequency. The deviation varies a lot for large frequency shifts, but for a small frequency range, this deviation is quite constant. For the range in which we measure, the deviation is about 250 Hz. Because the frequency itself is not really relevant, but more the change in frequency, there is no compensation for this.

7-2 Complete System Tests

After getting everything to work properly and tweak some values in some components, a full system check was made. The results of the tests can be found in table 7-1. The graphs obtained for every run can be found in figure 7-8. The implications of these graphs are discussed in chapter 8: Conclusion.

Table 7-1: Results of full system run

Thickness μm	Frequency (Arduino) kHz	Frequency (Oscilloscope) kHz	Bit used to generate frequency
0	37.0	37.04	147
40	36.71	36.76	142
80	36.57	36.5	140
420	38.87	38.76	179
780	36.4	36.5	135

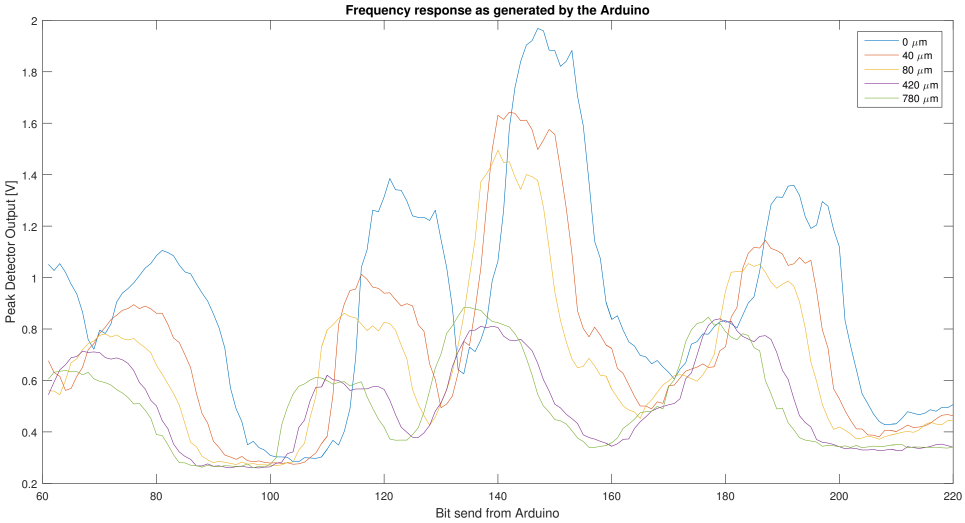

Figure 7-8: Graphs obtained after full system run.

Conclusion

The conclusion of this report is that an acoustic measuring principle is certainly possible. The first tests of trying to implement such a system were moderately successful.

The system is quite capable of putting a certain frequency on the piezo. The attempts of making the piezo input look like a sine wave were very successful. It still is not a perfect sine wave. This is especially noticeable at the output at which weird frequencies appear that do not appear when using a more perfect sine. The accuracy with which a specific frequency of the sinusoidal wave can be made is quite low. This is partly due to the fact that only 8 bits were used. With more bits, a higher accuracy could have been reached. Another part of the problem was that the frequency range the VCO could handle was very difficult to adjust. Having a couple of nanoFarads more of 1 specific capacitor would put the frequency range a couple of 100 kHz wider.

The system is quite capable of reading the attenuation of the received signal. The peak detector works excellent, even under low-amplitude conditions. The received value in the Arduino is a good reflection of the amplitude of the returned signal.

The Arduino is quite capable of determining a frequency coming from the VCO. The deviation was expected to be larger, but turned out to work properly in the end anyways.

The whole system functions moderately successful. For small layers, the output of the peak detector is higher, and the system has an easier way of determining the peak value. At higher grease layer thickness, the influence of resonance peaks in the vicinity is greater. In the final graph (figure 7-8) can be seen that the peak to the right is seen as "highest" peak (at 420 μm) and that frequency is chosen.

The performance of the system meets most specifications. The specifications which were not met, especially had to do with the accuracy of the system, as can be seen from the final table (table 7-1). The difference between 0 and 40 micron is 5 bits, an accuracy of about $\pm$ 4 μm. However, there are also 5 bits between 80 and 780 μm, which is an accuracy of $\pm$ 70 μm.

The sensor is able to be temperature dependent up to a certain degree. Since the frequency is checked by the Arduino itself, there is no frequency shift due to temperature. All other components are able to handle temperature differences between 20 and 85 degrees. Note that the electronics are also placed outside, so they probably will not reach extremely high temperatures. The properties of the grease itself will probably change with temperature though. This was not taken into account.

The design of the sensor is such that it does not impact the duct too much. It is also easily cleanable and therefore does not need to come into contact with the chemicals used by the cleaning company for the duct.

Discussion

There are a few considerations which can be made regarding improvements of the performance of the sensor. One of these considerations is the sheet thickness of the materials. If the sheet thickness reduces, less signal will be lost in the transfer of signal from piezo to piezo.

Another consideration can be to integrate the electronics part on a PCB and not on circuits board. In this design temperature influence has not been investigated but can have an effect on the system performance, because the properties of grease might change with temperature.

Another consideration regarding the whole system can be made with regards to the choice on the components. The VCO can become more accurate if the capacitance was changed or another VCO was used. The Arduino could also become more accurate by using more digital pins as input for the DAC, so a voltage can be created more accurately.

Furthermore, the sinusoidal signal generated by the LPF can be made to have less distortion. The received signal from the piezo will become more clean and easier readable by the Arduino. Lastly, a more precise and complex algorithm for finding the peaks of the receiving signal can be considered.

From another point of view, with the implementation of the system the responsibility of cleaning the extraction channel lies more with the cleaning company. The extraction channel poses a potential hazard, and the system currently does not inherently support any sharing of the responsibility of cleaning the channels.

References

[1] *Vetkanaal.nl | de specialist in het reinigen van vetkanalen*, https://www.vetkanaal.nl/, Jun. 2018.

[2] Elcometer, *Mtg4 material thickness gauge*, http://www.elcometerndt.com/en/precision-thickness/ptg8-precision-thickness-gauge/ptg8-precision-thickness-gauge.html, Accessed on April 25th 2018.

[3] L. A. V and S. D. W, "Duct grease deposit detection devices, systems, and methods", Granted Patent US 8487776 B2, Jul. 16, 2013. [Online]. Available: https://lens.org/061-952-189-984-841.

[4] Tompkins, H.G., Irene, E.A., *Handbook of Ellipsometry*. William Andrew, 2005. [Online]. Available: https://books.google.nl/books?id=6PQf1fSzHHEC&printsec=frontcover&hl=nl&source=gbs_ge_summary_r&cad=0#v=onepage&q&f=false.

[5] H. Fujiwara, *Spectroscopic Ellipsometry: Principles and Applications*. John Wiley & Sons, 2007. [Online]. Available: https://books.google.nl/books?hl=nl&lr=&id=tTMn0NKcpjsC&oi=fnd&pg=PR7&dq=ellipsometry&ots=NrPXtmTUqM&sig=0GE15sA9D9Yh7XdhEHP9lYLChwc#v=onepage&q=ellipsometrythickness&f=false.

[6] A. Franquet, J. D. Laet, T. Schram, H. Terryn, V. Subramanian, W. van Ooij, and J. Vereecken, "Determination of the thickness of thin silane films on aluminium surfaces by means of spectroscopic ellipsometry", *Thin Solid Films*, vol. 384, no. 1, pp. 37–45, 2001. [Online]. Available: http://www.sciencedirect.com/science/article/pii/S0040609000018058.

[7] F. Sagnard, F. Bentabet, and C. Vignat, "In situ measurements of the complex permittivity of materials using reflection ellipsometry in the microwave band: Experiments (part ii)", *IEEE Transactions on Instrumentation and Measurement*, vol. 54, no. 3, pp. 1274–1282, Jun. 2005, ISSN: 0018-9456. DOI: 10.1109/TIM.2005.847199.

[8] M. M. Shari, N. Buniyamin, and M. A. Halim, "Enhancement of an infrared based fat measurement sensor.", *Proc. of the IEEE International Conference on Smart Instrumentation, Measurement and Applications (ICSIMA)*, vol. 1, no. 1, pp. 1–6, 2013. DOI: 10.1109/ICSIMA.2013.6717973. [Online]. Available: https://ieeexplore.ieee.org/stamp/stamp.jsp?arnumber=6717973.

[9] J.-L. Lai, R.-S. Lin, and S.-C. Tsai, "Near-infrared optics bio-sensor used in body-fat measurement", *IEEE Transactions on Instrumentation and Measurement*, vol. 1, no. 1, pp. 1–4, 2016. DOI: 10.1109/ICASI.2016.7539813. [Online]. Available: https://ieeexplore.ieee.org/stamp/stamp.jsp?tp=&arnumber=7539813.

[10] P. D. J. McClements, "Analysis of lipids", *Department of Food Science*, section 5, 2003. [Online]. Available: http://people.umass.edu/~mcclemen/581Lipids.html.

[11] J. J. da Silva, A. M. N. Lima, F. H. Neff, and J. S. da Rocha Neto, "Non-invasive fast detection of internal fouling layers in tubes and ducts by acoustic vibration analysis", *IEEE Transactions on Instrumentation and Measurement*, vol. 58, no. 1, pp. 108–114, Jan. 2009, ISSN: 0018-9456. DOI: 10.1109/TIM.2008.927206.

[12] C. E. Brown and M. F. Fingas, "Development of airborne oil thickness measurements", *Marine Pollution Bulletin*, vol. 47, no. 9, pp. 485–492, 2003, ISSN: 0025-326X. DOI: https://doi.org/10.1016/S0025-326X(03)00203-0. [Online]. Available: http://www.sciencedirect.com/science/article/pii/S0025326X03002030.

[13] R. M. Bielemann, M. C. Gonzalez, T. G. Barbosa-Silva, S. P. Orlandi, M. O. Xavier, R. B. Bergmann, and M. C. F. Assuncao, "Estimation of body fat in adults using a portable a-mode ultrasound", *Nutrition*, vol. 32, no. 4, pp. 441–446, 2016, ISSN: 0899-9007. [Online]. Available: http://www.sciencedirect.com/science/article/pii/S0899900715004153.

[14] B.Kesil, D.Margulis, and E.Gershenzon, "Method and apparatus for measuring thickness of conductive films with the use of inductive and capacitive sensors", Granted Patent US6593738B2, Jul. 15, 2003. [Online]. Available: https://patentimages.storage.googleapis.com/d1/59/24/c2593f3976a979/US6593738.pdf.

[15] R. Igreja and C. Dias, "Analytical evaluation of the interdigital electrodes capacitance for a multi-layered structure", *Sensors and Actuators A: Physical*, vol. 112, no. 2, pp. 291–301, 2004, ISSN: 0924-4247. DOI: https://doi.org/10.1016/j.sna.2004.01.040. [Online]. Available: http://www.sciencedirect.com/science/article/pii/S0924424704000779.

[16] Z. Gang, X. Rui, and C. Yu, "Research on double coil pulse eddy current thickness measurement", *IEEE*, pp. 406–409, 2017. DOI: 10.1109/ICICTA.2017.97. [Online]. Available: https://ieeexplore.ieee.org/stamp/stamp.jsp?tp=&arnumber=8089980.

[17] T. Yasui, T. Yasuda, K.-i. Sawanaka, and T. Araki, "Terahertz paintmeter for non-contact monitoring of thickness and drying progress in paint film", *Appl. Opt.*, vol. 44, no. 32, pp. 6849–6856, Nov. 2005. DOI: 10.1364/AO.44.006849. [Online]. Available: http://ao.osa.org/abstract.cfm?URI=ao-44-32-6849.

[18] W.-L. Chen and Y.-C. Yang, "Inverse estimation for unknown fouling-layer profiles with arbitrary geometries on the inner wall of a forced-convection duct", *International Journal of Thermal Sciences*, vol. 49, no. 1, pp. 86–98, 2010, ISSN: 1290-0729. DOI: https://doi.org/10.1016/j.ijthermalsci.2009.06.005. [Online]. Available: http://www.sciencedirect.com/science/article/pii/S1290072909001446.

[19] J.N.Reddy, *Theory and Analysis of Elastic Plates and Shells*. CRC Press, 2006.

[20] *Physics*, https://physics.stackexchange.com/questions/90021/theory-behind-patterns-formed-on-chladni-plates, May 2017.

[21] *Arbitrary/function generators*, AFG3000C Series Datasheet, Tektronix, Sep. 2016.

[22] *Digital storage oscilloscopes*, TDS2000C Series Datasheet, Tektronix, Dec. 2016.

[23] *P5123 speaker specifications*, 2050000001338, Kemo electronic, May 2018.

[24] *The engineering toolbox*, https://www.engineeringtoolbox.com/sound-speed-solids-d_713.html, Jun. 2018.

[25] *Mc33078 dual high-speed low-noise operational amplifier*, MC33078 Datasheet, Texas Instruments, Nov. 2006.

[26] *Dac0800/dac0802 8-bit digital-to-analog converters*, DAC0800LCN/NOPB Datasheet, Texas Instruments, Feb. 2013.

[27] *High-speed cmos logic phase-locked loop with vco*, CD54HC4046A, CD74HC4046A, CD54HCT4046A, CD74HCT4046A, Texas Instruments, Dec. 2003.

[28] *Analysis of the sallen-key architecture*, Application report, Texas Instruments, Sep. 2002.

[29] *Arduino uno rev3*, https://store.arduino.cc/arduino-uno-rev3, Jun. 2018.

[30] *Atmega328/p*, Microcontroller Arduino Uno: The ATmega328/P Datasheet, Atmel, Nov. 2016.

Appendix

A-1 Matlab Code for Recording the Piezo Signal

This chapter shows which codes are used for the measurements and implementation of the acoustic sensor system.

A-1-1 Matlab Code for Recording Piezo Signal

This Matlab script describes how the signal from the receiving piezo is recorded.

Listing A.1: Code for recording piezo signal.

```
Fs = 192000;
sec = 130;
ruimte = 0.5;
presec = 1.5;
nbits = 16;
nchan = 2;
StartF = 1e3;
StopF = 15e3;
t = 0:1/Fs:sec;
r = audiorecorder(Fs, nbits, nchan, -1);
%pause(presec);
record(r, sec);
pause(sec);
stop(r);
y = getaudiodata(r);
% y1 = y(:,1);
% y2 = y(:,2);
%ytr = y(4e4:length(y));
%yfft = fftshift(abs(fft(y)));
%plot(yfft)
%N = length(yfft);
%fgrid = Fs*(-(N-1)/2:(N-1)/2)/(N);
%plot(fgrid,yfft)
```

A-1-2 Matlab Code for Phase and Attenuation Plots

In this section the Matlab code for the axis of the phase and attenuation of the piezo signal can be seen.

Matlab Code for Phase and Attenuation Response

This section describes the simulated lock-in amplifier described in section 5-6-1.

Listing A.2: Code for finding the phase and attenuation.

```
%ys = signal from dut
%yr = reference signal
nBits=16;
steps=2000;

ytot1=yr.*ys;
ytot2=hilbert(yr).*ys;

teller=1;
for a=1000:steps:length(ys)
    yft =fft(ytot1(a:a+steps),nBits);
    compa(teller)=yft(1);
    yft =fft(ytot2(a:a+steps),nBits);
    compb(teller)=yft(1);
    teller=teller+1;
end

plot(e,2*atan(abs(compa)./abs(compb)))
plot(e,sqrt(abs(compa).^2+abs(compb).^2))
```

Matlab Code for Axis of Plots

This Matlab script is used for the axis for phase and attenuation measurements.

Listing A.3: Code for axis of phase and attenuation plot.

```
teller=1;
steps=2000;
for a=1000:steps:length(yr)
    yft = fftshift(abs(fft(yr(a:a+steps))));
    N=length(yft);
    fgrid = Fs*(-(N-1)/2:(N-1)/2)/(N);
    [b,c] = max(yft);
    d(teller) = a;
    e(teller) = abs(fgrid(c));
    teller=teller+1;
end
```

A-2 C++ Code for Arduino

This section shows the Arduino code used for attenuation and frequency measurements, which are discussed in section 6-2-7.

Listing A.4: C++ code for Arduino

```
// defines for setting and clearing register bits
#ifndef cbi
#define cbi(sfr, bit) (_SFR_BYTE(sfr) &= ¬_BV(bit))
#endif
#ifndef sbi
#define sbi(sfr, bit) (_SFR_BYTE(sfr) |= _BV(bit))
#endif

void setup() {
  Serial.begin(9600);
  for(int i = 2; i < 11; i++) pinMode(i, OUTPUT);
}
void setprescale128(){
  sbi(ADCSRA,ADPS2) ;
  sbi(ADCSRA,ADPS1) ;
  sbi(ADCSRA,ADPS0) ;
}
void setprescale4(){
  cbi(ADCSRA,ADPS2) ;
  sbi(ADCSRA,ADPS1) ;
  cbi(ADCSRA,ADPS0) ;
}

void loop() {
  if(Serial.available()){
    int t = Serial.read() - 48;
    if(t == 0){
      double ret = findpeakfreq();
      Serial.print("Peak frequency at:");
      Serial.println(ret);
    }
    if(t==4){
      Serial.print("Frequency found:");
      Serial.println(makeFreqMeting(5000));
    }
    if(t>0 && t<4){
      int recint = getDatafromSerial(t);
      Serial.print("Recieved Variable:");
      Serial.println(recint);
      puttodigipins(recint);
    }
  }
}

double findpeakfreq(){
  int j = 0;
  double high = 0;
  int high2 = 0;
  for(j = 60; j < 220; j++){
```

```
    puttodigipins(j);
    delay(500);
    double temp = doanameas(100);
    Serial.println(temp);
    if(temp>high){
      high = temp;
      high2 = j;
    }
  }
  puttodigipins(high2);
  return makeFreqMeting(5000);
}

double doanameas(int lengthmeas){
  int q = 0;
  int amntsamp = 20;
  double totmeas = 0;
  for(q = 0; q< lengthmeas; q++){
    int k = 0;
  int readval[100];
  for(k = 0; k < amntsamp; k++){
    readval[k] = analogRead(5);
  }
  int tot = 0;
  for(k = 0; k < amntsamp; k++){
    tot = tot + readval[k];
  }
  double qwe = (double)tot/(double)amntsamp;
  totmeas = (q*totmeas+qwe)/(double)(q+1);
  }
  return totmeas;
}

int getDatafromSerial(int f){
  int delimiter = (int) '\n';
  int nothingrec = 0;
  String intData = "";

  for(int a = 0; a < f; a++){
    while(!Serial.available()){delay(1);}
    int ch = Serial.read();
    intData += (char) ch;
  }
  Serial.println(intData);
  if(f>0){
    byte intBuffer[4*f];
    int intLength = intData.length() + 1;
    intData.toCharArray(intBuffer, intLength);
    int digit = atoi(intBuffer);
    return digit;
  }
  return -1;
}

void puttodigipins(int toput){
  //Pin 13 as LSB / Pin 2 as MSB
  int i = 0;
```

```
  int pin = 10;
  int alm = 0;
  if(toput > 255) return;
  for(i = 128;; i=i/2){
    if(toput > i || toput == i){
      toput = toput-i;
      digitalWrite(pin,HIGH);
    }
    else{
      digitalWrite(pin,LOW);
    }
    pin = pin - 1;
    if(i<2) break;
  }
}

double makeFreqMeting(int times){
  setprescale4();
  double totfreq = 0;
  int timesrun = 0;

  while(timesrun<times){
  int lengthofr = 300;
  unsigned short recvalues[lengthofr];
  int time1 = 0;
  int time2 = 0;
  int i = 0;
  int high = 0;
  int pers = 0;
  double tottime=0;
  double freq=0;

  time1 = micros();
  for(i = 0; i < lengthofr; i++){
    recvalues[i] = analogRead(0);
  }
  time2 = micros();

  for(i = 0; i < lengthofr; i++){
     if(recvalues[i]>800 && high==0){
      pers++;
      high=1;
     }
     if(recvalues[i]<200 && high==1){
      pers++;
      high=0;
     }
  }
  tottime = (time2-time1) * 0.000001;
  freq = ((double)pers)/(2*tottime);
  totfreq = (totfreq*timesrun+freq)/(timesrun+1);
  timesrun++;
  }
  setprescale128();
  return totfreq;
}
```